Chalcogen Bonding Catalysis with Telluronium Cations

Robin Weiss, Emmanuel Aubert, Patrick Pale, Victor Mamane

RESEARCH ARTICLE

Chalcogen Bonding Catalysis with Telluronium Cations

Robin Weiss,[a] Emmanuel Aubert,[b] Patrick Pale,*[a] and Victor Mamane*[a]

[a] R. Weiss, Prof. P. Pale, Dr. V. Mamane
LASYROC, UMR 7177
University of Strasbourg
1 Rue Blaise Pascal, 67000 Strasbourg, France
E-mail: ppale@unistra.fr; vmamane@unistra.fr
[b] Dr. E. Aubert
CRM2
University of Lorraine
BP 70239, Boulevard des Aiguillettes, 54506 Vandoeuvre-lès-Nancy, France

Supporting information for this article is given via a link at the end of the document.

Abstract: Chalcogen bonding results from non-covalent interaction occurring between electrodeficient chalcogen atoms and Lewis bases. Among the chalcogens, tellurium is the strongest Lewis acid but Te-based compounds are scarcely used as organocatalyst. For the first time, telluronium cations demonstrated impressive catalytic property at low loading in three benchmark reactions: the Friedel-Crafts bromination of anisole, the bromolactonization of ω-unsaturated carboxylic acids and the aza-Diels-Alder between Danishefsky's diene and imines. The ability of telluronium cations to interact with a Lewis base through chalcogen bonding was demonstrated on the basis of multi-nuclear (^{17}O, ^{31}P and ^{125}Te) NMR analysis and DFT calculations.

Although known since 1783, tellurium only slowly gained interest.[1] It is employed in some alloys, solar panels and semiconductors. Its implication in organic chemistry is more diverse, owing to the special properties of this element.[2] Tellurium is the last stable element of the chalcogen group,[3] and as such, the largest[4] and the less electronegative,[5] that is the more polarizable and ionizable in this series. For these reasons, tellurium species exhibit the strongest non-covalent interaction with electron-rich atom through the so-called chalcogen bond (ChB), compared to their sulfur and selenium analogs.[6,7] ChBs are defined in analogy with halogen bonds (XB) as the interaction of an electron donor (Lewis base) with the electropositive region (σ-hole) located at the outermost end of a σ-bond including a chalcogen atom.[8]

ChB has been sparingly investigated in the last few decades and mostly in solid state.[9] Following the development of XB applications in biology[10] and organic chemistry,[11] ChBs have very recently raised increasing interest in organic chemistry, especially in anion recognition and transport as well as in organocatalysis.[12] In the latter growing area, mostly S and Se derivatives have so far been investigated.[13] Nevertheless, in 2018, Matile studied perfluorophenylselenide and telluride as ChB donors in chloride-binding catalysis (Sch. 1, up)[14] and more recently, Huber used a bidentate triazolium-based tellurium catalyst in the same reaction and in Michael reactions with indoles (Scheme 1, middle).[15] While working on this manuscript, Gabbaï very recently demonstrated that telluronium species can bind chloride and even act as chloride transporter.[16]

Engaged in XB and ChB study for applications in organocatalysis, we have recently designed new chiral catalysts.[17] To further explore this area and take benefit of the tellurium enhanced ChB property, we are currently designing tellurium-based catalysts. Inspired by the works of Lenardão[18] and Yeung[19] who demonstrated that selenonium could act as organic Lewis acid and promote reaction, we designed new telluronium salts and studied them, and we report here their ChB ability and *for the first time* the high efficiency of these telluronium species as organocatalysts in typical reactions (Sch. 1, bottom).

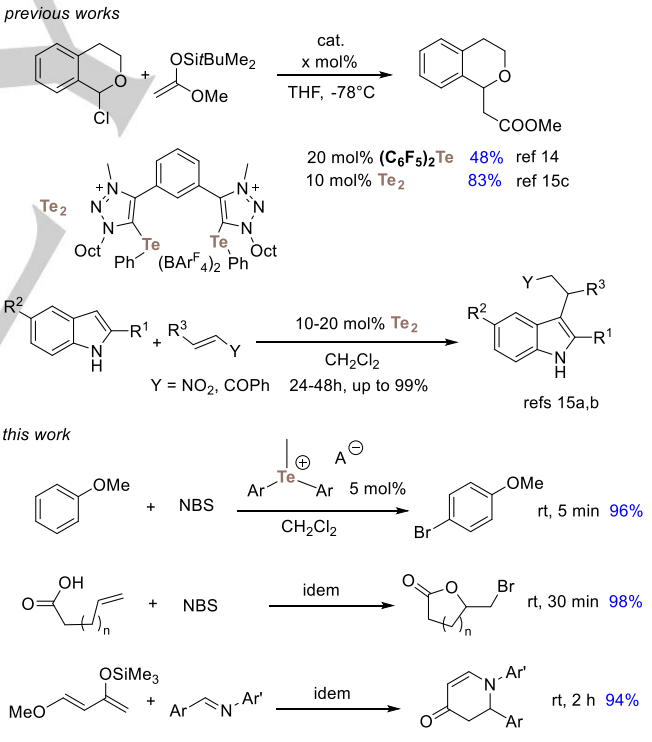

Scheme 1. Te-based organocatalysis: The two sole examples known and those described here.

To tune the expected ChB intensity, a series of telluronium derivatives carrying electron-rich or electron-poor substituent was prepared by alkylation of diaryltellurides. Addition of methyl triflate to diaryltellurides provided telluronium triflates but in modest yields (10-20%), while methyl iodide addition delivered unstable telluronium iodides. Adding silver triflate, tetrafluoroborate,

nitrate, or hexafluoroantimonate together with methyl iodide readily gave the corresponding telluroniums **1a-b**, **2a-b, 3a-b, 3d-e** and **4a-b** with excellent yields (Scheme 2). The tetrakis[3,5-bis(trifluoromethyl)phenyl]borate (BArF) telluroniums **1c, 2c, 3c, 4c** and tetrakis(pentafluorophenyl)borate telluronium **3f** were quantitatively obtained by anion metathesis from the corresponding triflates. They proved stable at room temperature for months as solids, except for **3d**, as well as in solution, except for **3e**, which slowly evolved to the starting diaryltelluride.[20] Among them, **3a** and **3e** provided suitable crystals for X-ray analysis, confirming the structures of these new telluronium salts.

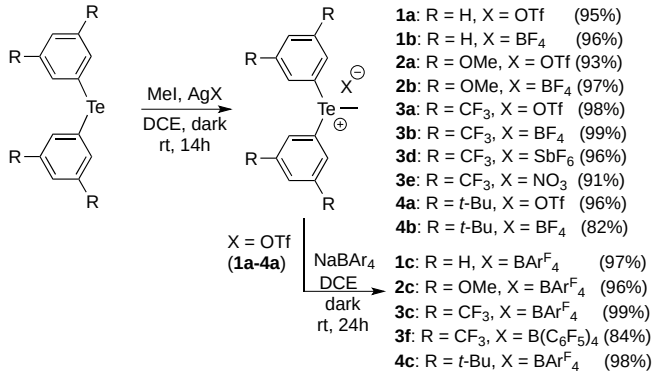

Scheme 2. Synthesis of the telluronium ChB donors.

In the solid state, **3a** and **3e** both crystallize with two independent cations in the asymmetric unit, all four molecules exhibiting a similar conformation (Fig. S9-S11 in S. I). In each structure, the telluronium cation exhibits close interaction with three neighbouring anions, one in each direction opposite to the C_{Ar}-Te and C_{Me}-Te bonds, almost aligned with the Te σ-holes (Fig. 1a). With anion-Te distances ranging from 2.831 to 3.048 Å, well below the sum of the van der Waals radii of the two elements (O 1.52 Å, Te 2.06 Å) and with a nearly linear arrangement of the TfO/NO$_3$••Te–C bonds (166 to 175°; Fig. S12-S15, S16-S17 and Table S10), these structures revealed the presence of ChB between each Te–C σ-hole and the non-bonding electrons of the triflate or nitrate oxygen atom (Fig. 1b).

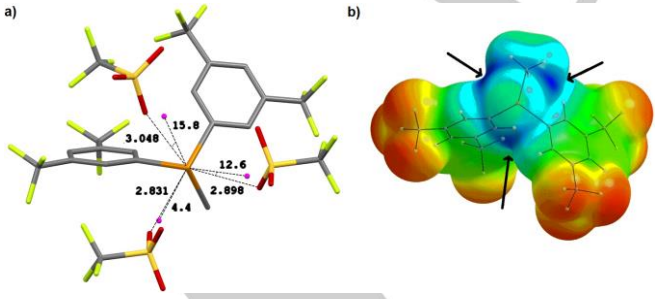

Figure 1. a) Molecular packing about tellurium Te1 in telluronium triflate **3a** (intermolecular Te···O bond distances in Å) and its superposition with the location of the ESP extrema ($V_{S,max}$, magenta dots; O···Te···$V_{S,max}$ angles are indicated in °); b) ESP map for the telluronium **3**$^+$ on DFT ρ=0.001 a.u. isodensity surface. Location of the three most positive extrema of ESP ($V_{S,max}$ points) are indicated with black arrows.

DFT calculations performed on the isolated telluronium cation **3**$^+$ confirmed the presence of three σ-holes along the three Te–C bonds, as shown by the positive electrostatic surface potential (ESP) around the tellurium centre (Fig. 1b). The corresponding $V_{S,max}$ values perfectly reflect the electron-withdrawing or donating properties of the substituent (Table S23), and as expected, the CF_3 group induces a significant increase ($V_{S,max}$ (kcal/mol): 130.3 (**3**$^+$) vs 113.0 (**1**$^+$) vs 103.2 (**2**$^+$)) deepening the σ-holes. The $V_{S,max}$ values of the two Te-Ar σ-holes are almost identical to one another whatever the telluronium, while the Te-Me σ-holes are always slightly lower. Superimpositions of the molecular packing around telluronium cations in **3a** and of the positions of the ESP extrema (Fig. 1a and S16-S17) show that the position of the anions is governed by the electrostatic interaction with the cation, guided through the three σ-holes that are responsible for the $V_{S,max}$ observed on the molecular surface.

Encouraged by these positive structural results, we further studied the telluronium ChB in solution. For that, ^{17}O-labelled Ph_3PO[21] was used as a probe in NMR, expecting that direct ^{17}O and ^{125}Te NMR monitoring of the interacting atoms would give key information on the interaction between the basic Ph_3PO oxygen atom and the Te σ-holes. Using a phosphine oxide as ChB acceptor could further allow ^{31}P NMR monitoring[22] Once added to a telluronium d^2-dichloromethane solution, Ph_3PO induced significant shifts of the ^{17}O, ^{31}P and ^{125}Te NMR signals (Table 1).

Table 1. ^{125}Te, ^{17}O and ^{31}P NMR chemical shift differences from telluronium salts **1**-**3** in the presence of Ph_3PO.[a]

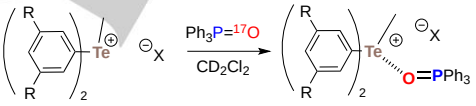

Entry	Telluronium (R, X)	^{125}Te Δδ[b]	^{17}O Δδ[c]	^{31}P Δδ[d]
1	**1a** (H, OTf)	2.08	0.57	6.71
2	**1b** (H, BF$_4$)	4.13	4.96	1.89
3	**1c** (H, BAr$^F_4$)	31.64	10.37	3.07
4	**2a** (OMe, OTf)	4.16	4.69	4.45
5	**2b** (OMe, BF$_4$)	4.10	5.03	1.65
6	**2c** (OMe, BAr$^F_4$)	29.90	9.69	3.78
7	**3a** (CF$_3$, OTf)	-3.13	4.47	0.98
8	**3b** (CF$_3$, BF$_4$)	-4.26	8.41	2.27
9	**3c** (CF$_3$, BAr$^F_4$)	11.62	21.10	6.83
10	**3d** (CF$_3$, SbF$_6$)	-4.65	7.25	3.17
11	**3e** (CF$_3$, NO$_3$)	6.33	2.21	0.70
12	**3f** (CF$_3$, B(C$_6$F$_5$)$_4$)	0.06	9.45	3.22
13	**4a** (*t*-Bu, OTf)	0.78	1.81	0.55
14	**4b** (*t*-Bu, BF$_4$)	1.50	2.09	0.66
15	**4c** (*t*-Bu, BAr$^F_4$)	24.48	5.04	2.41

[a] Conditions: 1:1 mixture (20 mM) of telluronium salts and Ph_3PO in CD_2Cl_2 at 25 °C; [b] δ_{Te} of the telluronium salts before and after addition of Ph_3PO are

given in S.I. (Tab. S1) as well as NMR incertitudes (Tab. S2); [c] δ_O in the presence of **1**-**4** (given in S.I. (Tab. S1) as well as NMR incertitudes (Tab. S4)) compared to δ_O of free Ph_3PO (47.41 ppm); [d] δ_P in the presence of **1**-**4** (given in S.I. (Tab. S1) as well as NMR incertitudes (Tab. S3)) compared to δ_P of free Ph_3PO (27.45 ppm).

Expected to be driven by Te σ holes deepness, the equilibrium occurring upon Ph_3PO addition should be affected by the electronic effect of the telluronium aryl substituent, but also by the ability of the anion to act as a Lewis base and thus to compete with the added $OPPh_3$. Such competition may be responsible for the variable peak broadening observed in some spectra for certain telluronium-$OPPh_3$ complexes.

Therefore, electronic effect should best be detectable if no competition for Te σ holes occurs. The telluronium series **1c**, **2c**, **3c** and **4c**, carrying the less coordinating anion BArF, was designed and prepared for these reasons in order to maximize Ph_3PO••Te interaction. Rewardingly, these BArF derivatives exhibited the largest NMR shifts (entries 3, 6, 9 and 15), whatever the measured nucleus. Furthermore, good correlations between Δδ and σ Hammett constants were obtained in ^{17}O and ^{31}P NMR (R^2 = 0.9375 and 0.9846 respectively; see Fig. S4). The latter clearly confirms the formation of Ph_3PO••Te complexes, and the role electronic effects played in this formation: the most effectively formed was obtained with the more electrodeficient telluronium **3**$^+$, the one having the largest σ holes (see $V_{s,max}$ values above), inducing the largest ^{17}O and ^{31}P NMR shifts.

Alternatively, the anion effect could be best evaluated within the telluronium series which exhibits the largest σ holes (see Table S21), i.e. the **3**$^+$ derivatives. Interestingly, the *a* index proposed by Alvarez to define the coordination ability of anions toward transition metal ions[23a] allowed to rationalize the observed Δδ variations. Remarkable correlations were indeed achieved with ^{17}O and ^{31}P NMR shifts for the **3a**-**3f** telluronium salt series (entries 7-12; see Fig. S5, R^2 = 0.9607 and R^2 = 0.9420 respectively). These results confirm that coordination of the telluronium counterions compete with Ph_3PO for the formation of Ph_3PO••Te complexes.

It is worth noticing that, although *a* values were reported for transition metals, lanthanides, and *s*-block metals,[23] the present correlations suggest that they are also well suited for telluronium cations.

In contrast to $\Delta\delta_O$ and $\Delta\delta_P$, only moderate to poor correlations could be achieved with $\Delta\delta_{Te}$, both for electronic and anion effects (see Fig. S6). This was expected because ^{125}Te NMR spectroscopy is highly sensitive to electronic and geometry changes in the tellurium environment.[24] Nevertheless, the correlation profile between $\Delta\delta_{Te}$ and *a* for the telluronium salt series **3**$^+$**X**$^-$ showed that $\Delta\delta_{Te}$ is differently influenced if the anion is well or poorly coordinating. Thus, by considering only low (BArF and BC_6F_5) and medium (SbF_6 and BF_4) coordinating anions, a very good correlation (R^2 = 0.9931) was obtained between $\Delta\delta_{Te}$ and *a*. With the more coordinating anions (NO_3 and TfO), the effect of Ph_3PO addition is balanced by other parameters, probably related to their competition for interaction with the telluronium and may be some modifications of the telluronium geometry if both the anion and Ph_3PO interact with.

A complementary analysis of ^{125}Te chemical shifts was performed by calculating the chemical shielding of the tellurium in telluronium cations **1**$^+$-**4**$^+$ (see S. I., section VII). Interestingly, the good linear correlation between the chemical shifts of telluroniums **1c-4c** measured in solution and the calculated chemical shielding of **1**$^+$-**4**$^+$ showed that the δ_{Te} trend in this series can be well reproduced by DFT calculations (R^2 = 0.9076, Fig.S18). This result confirmed that δ_{Te} in telluroniums **1c-4c** is mostly influenced by electronic parameters. However, no correlation was observed between the calculated chemical shielding and the measured δ_{Te} for the telluronium-$OPPh_3$ adducts (Fig. S20). This was expected because the measured δ_{Te} in solution corresponded to an equilibrium process whereas the chemical shielding were calculated for the adducts only.

It is interesting to note that the measured and calculated chemical shift values of the telluroniums reported here nicely fit with those recently reported (Fig. S19).[24d]

To further probe this Ph_3PO••Te interaction and to assess the formation of a monoadduct Ph_3PO--Te+, we performed NOESY experiment (Fig. S7) on the solution containing Ph_3PO and **3c**, the most effective salt for such complex formation (see above). This experiment clearly established the spatial proximity of *ortho* protons of Ph_3PO with the *ortho* protons of the 3,5-di(trifluoromethyl)phenyl group of the telluronium entity (Fig. 2a). Furthermore, nOe was also detected between the *ortho*-protons of Ph_3PO and the methyl group of the telluronium. Interestingly, calculations performed on a complex Ph_3PO-**3**$^+$ also highlighted the proximity of these protons (Fig. 2b and S25), with a very short distance between Te and O (2.570 Å), in line with the strongest ^{17}O NMR shift (Δδ 21.1 ppm) observed with this complex. Its formation was further confirmed by *in situ* mass spectrometry, which allowed to detect the species present in the corresponding solution with a mass peak at 849.0448 within a set of peaks typical for the isotopic distribution of a 1:1 adduct between **3c** and Ph_3PO (Fig. 2c and S8).

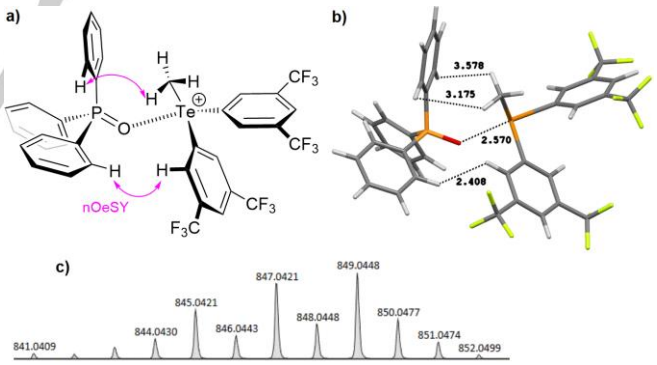

Figure 2. a) Representation of the interactions between $OPPh_3$ and the telluronium protons of **3c** as suggested from ^{17}O, ^{31}P and ^{125}Te NMR and NOESY experiment (only one single hydrogen was highlighted for clarity); b) B3LYP-D3/Def2TZVPP calculations of the **3**$^+$-Ph_3PO complex; c) mass spectrum of the **3**$^+$-Ph_3PO complex.

Overall, these effects established the presence of a ChB between Te and O of Ph_3PO through interaction of the latter with the aryl-Te σ-hole located between the telluronium methyl and the other aryl group, as schematically shown in Fig. 2a.

As these observations clearly showed the Lewis acidity of the cationic chalcogen and its ability to activate a carbonyl-type derivative, it was worth evaluating their propensity to act as

catalyst in some reactions. The bromination of anisole with *N*-bromosuccimide (NBS) was first used as benchmark reaction with catalysts **1**-**3** (Table 2). Interaction of the NBS carbonyl with the Te σ-hole should lower the N-Br bond LUMO and favour its attack by the electron-rich aromatic moiety of anisole.

At room temperature, no reaction occurred without telluronium (entry 1), but in the presence of catalytic amount of it (5 mol%), anisole bromination was achieved within 5 min. All the telluronium salts gave the expected 4-bromoanisole in high yields and no significant difference was noted between TfO and BF_4 anions. As expected from the preceding studies, the BArF telluroniums **1c**, **2c** and **3c** provided the best results, giving within 5 min the brominated product in high yields and almost quantitatively with **3c** as catalyst (entries 4, 7 and 10). Based on these results and on the higher $V_{s,max}$ values (Table S23), catalyst **3c** was used for further catalytic tests (entries 11-15) and for other reactions (Tables 3 and 4). Increasing or decreasing the catalyst amount did not change the catalyst efficiency (entries 11, 12 vs 10), and interestingly, as low as 0.5 mol% of catalyst still very efficiently promoted this reaction within 5 min. (entry 13). The catalyst **3c** was then evaluated in competition with chloride, known to strongly interact with Te species.[7a,15a,16,25] Accordingly, the catalytic activity of **3c** was suppressed in the presence of an equivalent amount of tetrabutylammonium chloride (entry 14). The possibility of hidden Brønsted catalysis was ruled out by adding potassium carbonate which did not modify the reaction course and its yield (entry 15). It is worth to mention that this reaction could be performed at mmol scale without significant change (entry 10[f]). The catalyst stability was also attested by NMR monitoring of the reaction; ^1H and ^{19}F NMR confirmed the structural integrity of the catalyst after reaction (see S.I. p 31-33).

Table 2. Bromination of anisole catalyzed by telluroniums.

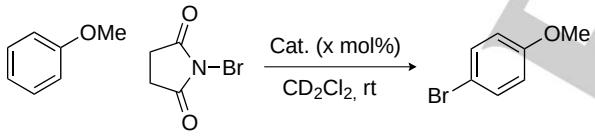

Entry[a]	Catalyst		loading	Yield (%)[b]
1	None			0
2	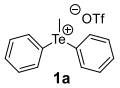	**1a**	5 mol%	79[c]
3	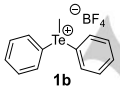	**1b**	5 mol%	86
4	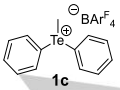	**1c**	5 mol%	89
5		**2a**	5 mol%	84
6	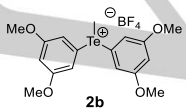	**2b**	5 mol%	81
7	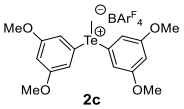	**2c**	5 mol%	87
8	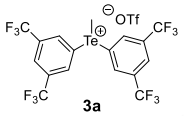	**3a**	5 mol%	82
9	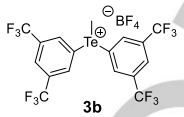	**3b**	5 mol%	87
10	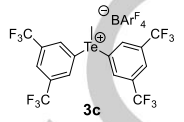	**3c**	5 mol%	96 (94)[f]
11		**3c**	10 mol%	96
12		**3c**	1 mol%	97
13		**3c**	0.5 mol%	97
14[d]		**3c**	1 mol%	0
15[e]		**3c**	1 mol%	98

[a] Reactions were carried out with anisole (0.054 mmol), catalyst and NBS (0.056 mmol) in CD_2Cl_2 at rt for 5 min.; [b] Determined by ^1H NMR (see SI for details, NMR yield incertitude: ± 5%); [c] The same yield was obtained with **1a** synthesized directly from MeOTf, thus ruling out catalysis by silver salts; [d] In the presence of 1 mol% of nBu$_4$NCl after 24h; [e] In the presence of 10 mol% of K_2CO_3 after 5 min; [f] Isolated yield in brackets for a reaction performed at 1 mmol scale.

As NBS was efficiently activated by the telluronium catalyst in the aryl bromination described above, it seemed worth to examine another classical reaction induced by NBS, the bromolactonization reaction. A series of ω-unsaturated carboxylic acids was submitted to NBS in the presence of telluronium catalyst **3c** (Table 3). Rewardingly, the expected bromolactones were obtained within 30 min in good to quantitative yields for 4 to 6 membered rings (entries 1-8), but in lower yields for larger rings (entries 9-10), while no reaction occurred without catalyst (entry 1). The γ-lactone was quantitatively formed (entries 5-6), even with only 1 mol% of catalyst (entry 5) but higher catalyst loading proved necessary for efficiently producing the β- or δ-lactones, (entries 3-4 and 7-8 vs entry 5). For each case, the observed regioselectivity corresponds to what is expected from Baldwin 'rules'.[26] Here again, the reaction could be performed at mmol scale without significant change (entry 6[d]) and the catalyst remained stable during the reaction (see S.I. p 31-33), despite the role Lewis bases could play in bromo- and iodolactonisation.[27]

Table 3. Bromolactonisation catalyzed by telluronium.

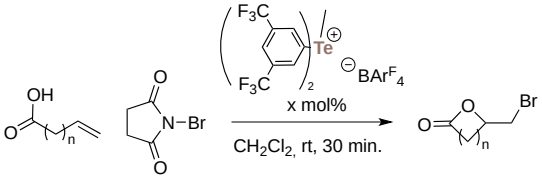

Entry [a]	Alkene	x	Lactone	Yield[b,c]

1	n = 1	0	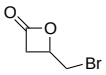	0
2		1		29 (26)
3		5		70
4		10		77 (68)
5	n = 2	1	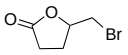	100 (98)
6		5		99 (92) [d]
7	n = 3	5	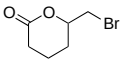	62
8		10		82
9	n = 4	5	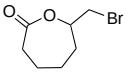	32
10	n = 8	5	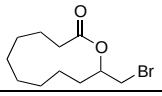	29

[a] Reactions were carried out with ω-unsaturated carboxylic acid (0.23 mmol), catalyst and NBS (0.23 mmol) in CH_2Cl_2 at rt for 30 min.; [b] Determined by ^{1}H NMR (see SI for details, NMR yield incertitude: ± 5 %); [c] Isolated yield in bracket; [d] reaction performed at 1 mmol scale.

In order to further illustrate the σ-hole catalytic property of telluronium species, we evaluated the ability of the telluronium **3c** to catalyze aza-Diels-Alder-type reaction. As an archetypal reaction, the Danishefsky's diene condensation with various imines was investigated (Table 4). Such reaction is known to follow a step-wise mechanism with soft Lewis acids or in protic solvents, driven by *N*-coordination or protonation.[28] Therefore, the soft telluronium **3c** should here similarly activate the imine and induce Mannich-type addition of the Danishefsky's diene. All the examined imines readily afforded the expected *N*-phenyl 2,3-dihydro-4-pyridinones in good to high yields with only 1 mol% of catalyst within 2 h at room temperature (entries 1, 3, 7). As expected, higher catalyst loading further improved the catalysis efficiency (entry 5 vs 4) and up to 91% of adducts could be obtained with 10 mol% of catalyst (entry 6 vs 4). Longer reaction times did not much improve yields (entries 2 vs 1, 4 vs 3 and 8 vs 7). A slight electronic effect was observed, with electron-poor imine being less reactive (entries 7,8) as expected from the envisaged mechanism. As in the preceding reactions, the reaction could be performed at mmol scale (entry 6[d]) and the catalyst stability could be assessed by ^{1}H and ^{19}F NMR (see S.I. p 31-33).

Table 4. Telluronium-catalyzed condensation of imines with the Danishefsky's diene.

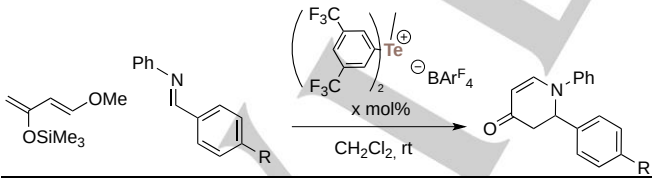

Entry [a]	Imine	Catalyst loading	Time	Yield[b,c]
1	R = H	1 mol%	2 h	87 (84) (76) [d]
2	"	1 mol%	24 h	87
3	R = OMe	1 mol%	2 h	73
4	"	1 mol%	24 h	78 (73)
5	"	5 mol%	24 h	87
6	"	10 mol%	24 h	91 (88)
7	R = NO_2	1 mol%	2 h	60
8	"	1 mol%	24 h	64 (56)

[a] Reactions were carried out with imine (0.14 mmol), Danishefsky's diene (0.18 mmol) and catalyst in CH_2Cl_2 at rt for 2 h; [b] Determined by ^{1}H NMR (SI for details, NMR yield incertitude: ± 5 %); [c] Isolated yield in bracket; [d] reaction performed at 1 mmol scale.

In conclusion, after having prepared new telluronium salts, we demonstrated the presence of three σ-holes on these telluronium and their importance in solution as indicated by Ph_3PO binding studies through ^{17}O, ^{31}P and ^{125}Te NMR. The enhanced properties of these telluronium salts could be readily translated *for the first time* into high catalytic performance. These telluronium salts, especially the BArF telluronium carrying electron-withdrawing groups (**3c**), were able to efficiently catalyze various reactions, even at low loading. Quantitative reactions were thus achieved in the bromination of aromatic and in bromolactonization with only 0.5 mol% of catalyst. Aza-Diels-Alder-type reactions were also very effective (up to 90%) with 5 mol% of catalyst. The versatility of telluronium salts in their applications uncovered here opens up new routes/strategies in organic syntheses. Further works in those area are underway in our group.

Acknowledgements

This research was funded by the International Center of Frontier Research in Chemistry (icFRC), the LabEx CSC (ANR-10-LABX-0026 CSC). RB thanks the LabEx CSC, Strasbourg, for a PhD fellowship. The EXPLOR mesocenter is thanked for providing access to their computing facility (project 2019CPMXX0984/wbg13).

Keywords: chalcogen bonding • non-covalent interactions • organocatalysis • tellurium • Lewis acid

[1] a) J. Ibers, *Nature Chem.* **2009**, *1*, 508; b) J. V. Comasseto, *J. Braz. Chem. Soc.* **2010**, *21*, 2027–2031.

[2] N. Petragnani, H. A. Stefani, *Tellurium in Organic Synthesis*, 2nd Ed., Academic Press-Elsevier, Londres-Amsterdam, **2007**.

[3] The latest element of this series, polonium, is radioactive, with a half-live of 138 days for the α-emitting ^{210}Po isotope and 128 years for the ^{209}Po isotope. Nevertheless, tellurium also contains 2 radioactive isotopes with very long half-life (>9 10^{16} years).

[4] Atomic radius of this series (Å): O 0.66, S 1.04, Se 1.17, Te 1.37.

[5] Pauling electronegativity: O 3.5, S 2.5, Se 2.4, Te 2.1.

[6] T. Chivers, R. S. Laitinen, *Chem. Soc. Rev.* **2015**, *44*, 1725–1739.

[7] For recent examples, see: a) E. Navarro-Garcia, B. Galmès, M. D. Velasco, A. Frontera, A. Caballero, *Chem. Eur. J.* **2020**, *26*, 4706–4713; b) S. Mehrparvar, C. Wölper, R. Gleiter, G. Haberhauer, *Angew. Chem. Int. Ed.* **2020**, *59*, 17154–17161; *Angew. Chem.* **2020***, 132,* 17303–17311.

[8] Aakeröy, C. B.; Bryce, D. L.; Desiraju, G. R.; Frontera, A.; Legon, A. C.; Nicotra, F.; Rissanen, K.; Scheiner, S.; Terraneo, G.; Metrangolo, P.; Resnati, G. Pure Appl. Chem. 2019, 91, 1889-1892.

[9] P. Scilabra, G. Terraneo, G. Resnati, *Acc. Chem. Res.* **2019**, *52*, 1313–1324.

[10] G. Berger, P. Frangville, F. Meyer, *Chem. Commun.* **2020**, *56*, 4970–4981.

[11] R. L. Sutar, S. M. Huber, *ACS Catal.* **2019**, *9*, 9622–9639.

[12] a) L. Vogel, P. Wonner, S. M. Huber, *Angew. Chem. Int. Ed.* **2019**, *58*, 1880–1891; b) N. Biot, D. Bonifazi, *Coord. Chem. Rev.* **2020**, *413*, 213243.

[13] a) J. Bamberger, F. Ostler, O. García Mancheño, *ChemCatChem* **2019**, *11*, 5198–5211; b) M. Breugst, J. J. Koenig, *Eur. J. Org. Chem.* **2020**, 5473–5487.

[14] S. Benz, A. I. Poblador-Bahamonde, N. Low-Ders, S. Matile, *Angew. Chem. Int. Ed.* **2018**, *57,* 5408–5412.

[15] a) P. Wonner, A. Dreger, L. Vogel, E. Engelage, S. M. Huber, *Angew. Chem. Int. Ed.* **2019**, *58*, 16923–16927; b) P. Wonner, T. Steinke, L. Vogel, S. M. Huber, *Chem. Eur. J.* **2020**, *26*, 1258–1262; c) T. Steinke, P. Wonner, E. Engelage, S. M. Huber, *Synthesis* **2021**, DOI: 10.1055/a-1372-6309.

[16] B. Zhou, F. Gabbai. *Chem. Sci.* **2020**, *11,* 7495–7500.

[17] a) R. Weiss, E. Aubert, P. Peluso, S. Cossu, P. Pale, V. Mamane, *Molecules* **2019**, *2*4, 4484; b) V. Mamane, P. Peluso, E. Aubert, R. Weiss, E. Wenger, S. Cossu, P. Pale, *Organometallics* **2020**, *39*, 3936–3950.

[18] E. J. Lenardão, J. d. O. Feij, S. Thurow, G. Perin, R. G. Jacob, C. C. Silveira, *Tetrahedron Lett.* **2009**, 50, 5215–5217.

[19] X. He, X. Wang, Y-L. Tse, Z. Ke, Y-Y.Yeung, *Angew. Chem. Int. Ed.* **2018**, *57,* 12869–12873; *Angew. Chem.* **2018**, *130*, 1305–13055.

[20] N. S. Dance, W. R. Mc Whinnie, J. Mallaki, Z. Monsef-Mirzai, *J. Organomet. Chem.* **1980**, *198*, 131–143.

[21] Z. Deng, J.-H. Lin, J.-C. Xiao, *Nature Comm.* **2016**, *7*, 10337.

[22] Y.-P. Chang, T. Tang, J. R. Jagannathan, N. Hirbawi, S. Sun, J. Brown, A. K. Franz, *Org. Lett.* **2020**, *22*, 6647–6652.

[23] a) R. Diaz-Torres, S. Alvarez, *Dalton Trans.* **2011**, *40*, 10742–10750; b) S. Alvarez, *Chem. Eur. J.* **2020**, *26*, 4350–4377; c) *a* values for the considered anions: NO_3^- 0.0; TfO^- -0.4; SbF_6^- -1.0; BF_4^- -1.1; $B(C_6F_5)_4^-$ -1.9; BArF -3.4.

[24] a) M. J. Collins, J. A. Ripmeester, J. F. Sawyer, *J. Am. Chem. Soc.* **1988**, *110*, 8583–8590; b) M. R. Detty, W. C. Lenhart, *Organometallics* **1989**, *8*, 861–865 and 866–870; c) E. Pietrasak, A. Togni, *Organometallics* **2017**, *36,* 3750–3757. d) E. Pietrasak, C. P. Gordon. C. Coperet, A. Togni, *Phys. Chem. Chem. Phys.* **2020**, *22*, 2319–2326.

[25] a) G. E. Garrett, G. L. Gibson, R. N. Straus, D. S. Seferos, M. S. Taylor, *J. Am. Chem. Soc.* **2015**, *137*, 4126–4133; b) J. Y. C. Lim, J. Y. Liew, P. D. Beer, *Chem. Eur. J.* **2018**, *24*, 14560–14566.

[26] J. E. Baldwin, *J. Chem. Soc., Chem. Commun.* **1976**, 734–736.

[27] S. E. Denmark, M. T. Burk, *Proc. Nat. Acad. Sci. USA* **2010**, *107*, 20655-20660.

[28] a) S. Hermitage, D. Jay, A. Whiting, *Tetrahedron Lett.* **2002**, *43*, 9633–9636; b) S. Hermitage, J. A. K. Howard, D. Jay, R. G. Pritchard, M. R. Probert, A. Whiting, *Org. Biomol. Chem.* **2004**, *2*, 2451–2460; c) Y. Yuan, X. Li, K. Ding, *Org. Lett.* **2002**, *4*, 3309–3311.

[29] CCDC 2048353 and 2048354 contain the supplementary crystallographic data for this paper. These data are provided free of charge by The Cambridge Crystallographic Data Centre.

Entry for the Table of Contents

Taking benefit of Te chalcogen bonding: New telluroniums salts exhibit enhanced properties, due to the presence of 3 σ-holes, and highlighted in solution by Ph_3PO binding studies through ^{17}O, ^{31}P, ^{125}Te NMR, MS and NOESY. These enhanced ChB properties translated into high catalytic performance, with low loading (0.5-5 mol%), short reaction time (5 min-2 h) and high yields.